High critical current density and vortex pinning of epitaxial MgB_2 thin films

S. Y. Xu,[1,*] Qi Li,[1,2] E. Wertz,[1] Y. F. Hu,[1] A. V. Pogrebnyakov,[1] X. H. Zeng,[1] X. X. Xi,[1,2,3] and J. M. Redwing[2,3]
[1]*Department of Physics, The Pennsylvania State University, University Park, Pennsylvania 16802, USA*
[2]*Materials Research Institute, The Pennsylvania State University, University Park, Pennsylvania 16802, USA*
[3]*Department of Materials Science and Engineering, The Pennsylvania State University, University Park, Pennsylvania 16802, USA*
(Received 13 March 2003; published 5 December 2003)

We have studied transport properties of a number of *in situ* epitaxial MgB_2 thin films grown by hybrid physical-chemical vapor deposition. The films show single-crystal-like structure with a high T_c, a narrow ΔT_c and a high zero-field j_c. The best $j_c(H=0)$ of the films at 5 K is comparable to the estimated depairing current density j_0 of MgB_2. The zero-field $j_c(T)$ data of different films can be scaled to $j(t)=(1-t^2)^{\alpha}(1+t^2)^{1/2}$, where $j(t)=j_c(t)/j_c(0)$ and $t=T/T_c$. We have found that $\alpha=1.7\pm0.1$ fits the data measured with the 4-probe method and $\alpha\sim2$ fits the data derived from the magnetization hysteresis *M-H* measurements. At low temperature the $j_c(H)$ of the films show a common feature that $j_c(H)$ first appears as a plateau when the external field is lower than H^*, where $\mu_0 H^*\sim10^{-2}$ T, and then $j_c(H)\propto H^{-\beta}$ when the field is lower than a crossover value $\mu_0 H_m\sim1$ T, where $\beta\sim0.7$–1.0 resembling that of epitaxial high-T_c cuprate films. Above H_m, $j_c(H)$ decreases steeply. These results may be associated with the columnar growth mode of the films, where strong pinning centers are mainly located at the column boundaries or twin boundaries, and within a single-crystal-like column the pinning is weak. At low temperature, nearly temperature independent small peaks and flip-over in *M-H* loops are observed in the films, consistent with the high thermal activation energy $U_0(H,T)$ values calculated from the resistivity measurement of the films.

DOI: 10.1103/PhysRevB.68.224501 PACS number(s): 74.25.Fy, 74.25.Qt, 74.62.Bf, 74.78.Db

I. INTRODUCTION

The dependence of the critical current density j_c on temperature and magnetic fields is an important aspect of a superconducting material for both academic research and device applications. Among different types of superconducting materials, epitaxial thin films usually have a much better intergrain conductance than that of sintered bulk materials, but also more vortex pinning centers than those in single crystals. Both conditions favor a high j_c. For example, high-T_c $YBa_2Cu_3O_{7-\delta}$ (YBCO) thin films can show a zero-field j_c of 10^6–10^7 A/cm^2 at 77 K, or 10^7–10^8 A/cm^2 at 4.2 K; both are 2–3 orders of magnitude higher than that obtained in YBCO bulks or single crystals. Similarly, in the superconductor MgB_2 (Ref. 1) j_c values over 10^7 A/cm^2 in zero-field have been repeatedly obtained in thin films synthesized by two-step methods with post-annealing,[2,3] and recently by the *in situ* hybrid physical-chemical vapor deposition (HPCVD) approach.[4–6] The j_c of 3.5×10^7 A/cm^2 at 4.2 K in zero external field and 1×10^6 A/cm^2 at 20 K in 1 T of perpendicular field ($H\|c$) obtained from an *in situ* epitaxial MgB_2 film on 6H-SiC made by HPCVD method[5] is 1–3 orders of magnitude higher than that observed in MgB_2 sintered bulks, single crystals, wires or tapes.[7] This makes MgB_2 thin films promising for applications in many kinds of film-based passive and active devices working at the temperature range of 20–25 K, where an electrical cryostat could replace liquid helium cooling.[8]

To further increase the j_c value and improve the sustainability of MgB_2 thin films in fields, which is currently a common drawback of MgB_2 materials, it is necessary to have a clear picture of the vortex state and pinning mechanism in the films. In MgB_2 thin films with randomly oriented polycrystalline grains,[9] or films with a *c*-axis texture but random grain orientation in *ab* plane,[2] vortices seem to be mainly pinned by point defects.[9–11] The vortex glass model was suggested to describe the vortex state in these films.[12,13] Large suppression of j_c induced by flux jump at low temperature and low field was also observed in these films,[14] and quantum effects such as quantum fluctuation and tunneling of vortices are suggested to explain the large separation between irreversibility field $H_{\rm irr}$ and the upper critical field H_{c2} at low temperatures.[15] In the *in situ* epitaxial MgB_2 thin films made by HPCVD[4–6] and the films made by radio frequency sputtering followed with Mg diffusion processing,[16] both *c*-axis orientation and good in-plane epitaxy have been obtained, therefore one may expect a different vortex pinning mechanism in these films from those previously reported. In this paper, we present experimental data on the transport properties measured from over two dozen of MgB_2 thin films made by HPCVD, with an emphasis on the dependence of j_c on temperature and magnetic fields. The values of j_c were obtained by means of both 4-probe method as well as magnetization hysteresis loop *M-H* approach. As the MgB_2 films discussed in this paper consist of single-crystal-like columns with uniform column size,[4,17] bearing some similarity to that of high-quality epitaxial high-T_c cuprate (e.g., YBCO) thin films, we will discuss the vortex pinning in the films with some frameworks applied to high-T_c cuprate thin films.

II. EXPERIMENT

The fabrication procedures for the *in situ* epitaxial MgB_2 thin films by HPCVD have been described elsewhere in detail.[4–6] The films for this study were deposited at 710–760 °C on (0001) sapphire and 4H- or 6H-SiC single-crystal substrates (size $\sim5\times5$ mm^2) with a B_2H_6 flow rate of

25–50 sccm, yielding a deposition rate of 2–4 Å/s. The as-deposited films consist of hexagonal columns of pure superconducting phase MgB_2. Impurities such as MgO are only found in the film-substrate interface or on the film surface. From x-ray θ-2θ scan and φ-scan diffraction analyses, the films are single-crystal-like showing excellent crystalline texture and a perfect in-plane epitaxy with their *c*-axis perpendicular to the substrate surface.[5] The *ab* axes of the MgB_2 film grown on SiC follow the *ab* axes of the SiC as their lattices match well.[5] On sapphire, the majority of the MgB_2 film structures twist their *ab* axes in-plane by 30° with respect to the *ab* axes of sapphire to reduce the lattice mismatch between them, but a small portion of MgB_2 lattices have their *ab* axes following the *ab* axes of the sapphire substrate, yielding 30° twin boundaries.[5] The film surfaces are nearly free of big particles or outgrowths, and have a root-mean-square roughness $(R_q) \sim 4$ nm on both substrates.[4,17]

For j_c measurements with the 4-probe method, the films were patterned into bridges with a width of 20 to 50 μm and a length-to-width ratio of 2–20 via photolithography and Ar ion-beam milling. During ion milling, the samples were cooled with a liquid nitrogen stage to avoid processing damage. For magnetization measurement, the films were cut into $\sim 2.5 \times 5\ \mathrm{mm}^2$. Both the transport and magnetization *M-H* hysteresis loop measurements were performed on a Quantum Design Model 6000 Physical Property Measurement System with an accuracy of ± 0.01 K for temperature control and a maximum field of 9 T. Standard 4-probe current-voltage (*I-V*) measurements were performed. A criterion of 1 μV was used to determine the samples' critical current I_c from the *I-V* curves. In *M-H* loop measurements, a field-sweeping rate, $\mathrm{d}(\mu_0 H)/\mathrm{d}t$, of 2–10 mT/s was used, and at each fixed magnetic field, the magnetization value of the sample was averaged from 10 consecutive measurements.

III. RESULTS AND DISCUSSION

A. General transport properties

The as-deposited *c*-axis MgB_2 thin films typically show transition temperature T_c and width $\Delta T_c(10-90\,\%)$ of 39–41 K and 0.1–0.3 K, respectively. The residual resistance ration $RRR = \rho(300\ \mathrm{K})/\rho_n$ of the samples ranges from 2 to 30, where ρ_n is the residual resistivity near T_c.[4,6,18] Usually the films on SiC have a higher T_c than those on sapphire.[18]

We performed resistivity-temperature (ρ-*T*) measurements in varied external fields on both unpatterned films and patterned micro-bridges. Figure 1 plots the $\rho(T,H)$ data measured in parallel ($H \| ab$) and perpendicular ($H \| c$) fields for a $\sim$92 nm thick film on 6H-SiC from a $50\ \mu\mathrm{m} \times 1$ mm bridge with a measuring current density of 100 A/cm^2. In zero external field, this bridge sample shows $T_c \sim 40.3$ K, $\Delta T_c \sim 0.2$ K, ρ_n (at 41 K) $\sim 4\ \mu\Omega$ cm and $RRR \sim 5$. Note that in parallel fields $\Delta T_c(H)$ increases to $\sim$1.7 K at 9 T, while in perpendicular fields it increases faster to $\sim$5.4 K at 5 T. In terms of the transition width, the results are comparable to that observed in MgB_2 single crystals,[19,20] indicating

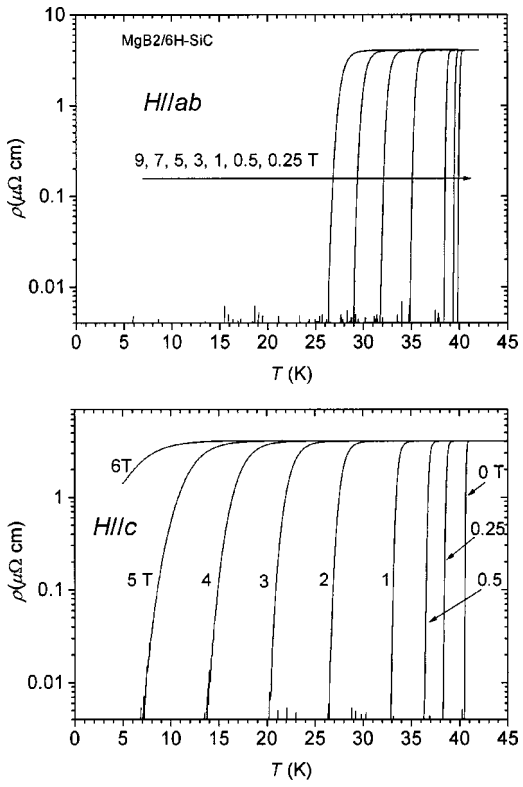

FIG. 1. Resistivity-temperature data measured in parallel ($H \| ab$) and perpendicular ($H \| c$) fields from a microbridge patterned in a 92 nm thick *in situ* epitaxial MgB_2 film grown on (0001) 6H-SiC substrate.

a high purity of the MgB_2 superconducting phase and perfect crystalline lattices. From the $\rho(T,H)$ curves we estimated the values of upper critical fields $\mu_0 H_{c2}(T)$ in both parallel and perpendicular configurations. Similar to the results reported in bulks, thin films and single crystals,[7,21] the $\mu_0 H_{c2}(0)$ values of the present films vary largely in both parallel and perpendicular fields, e.g., 6–23 T for $\mu_0 H_{c2}(0)$ in perpendicular fields, showing a strong sample dependence. As a general trend of these samples, the film with better single-crystal-like crystalline structure has lower $H_{c2}(0)$.

The j_c values measured from the samples appear to be dependent on the measurement methods applied. As shown in Fig. 2, by using *M-H* loop method and the expression derived from Bean critical state model, $j_c = 20\Delta M/a(1 - b/3a)$, where ΔM is the width of *M-H* loop, and *a* and *b* are the length and width of the sample (perpendicular to the applied field), respectively, we derived a nominal j_c value of 1.05×10^8 A/cm^2 at 5 K in zero external field for a film on 6H-SiC. For the same sample measured with 4-probe method, the j_c at 4.2 K is 3.5×10^7 A/cm^2 in zero external field. The main reason for the difference is that the Bean model is a first order approximation and the *M-H* measurement is an average result of the whole film, while the 4-probe method measures the properties of the weakest region of a microbridge sample. In addition, damage induced by lithography processing, the geometric effects[22,23] and self-field induced in microbridges can also cause the j_c measured to be lower than the real value. However, at zero external

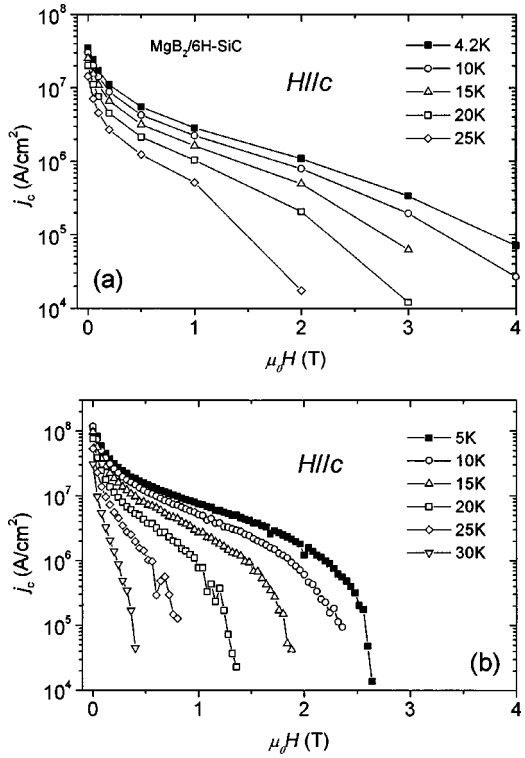

FIG. 2. Critical current density j_c in perpendicular field for a sample on 6H-SiC: (a) data measured with 4-probe method on a 30 μm wide bridge, and (b) data derived from *M-H* hysteresis loops with Bean critical state model.

field, the data obtained from both methods show a similar trend in the j_c-T curves as typically shown in Fig. 3: a positive curvature at $T \rightarrow T_c$, a nearly linear part in the central range of temperature and a negative curvature when $T \rightarrow 0$ K. In particular, most samples show a quite wide temperature range for the linear part in their zero-field j_c-T curves.

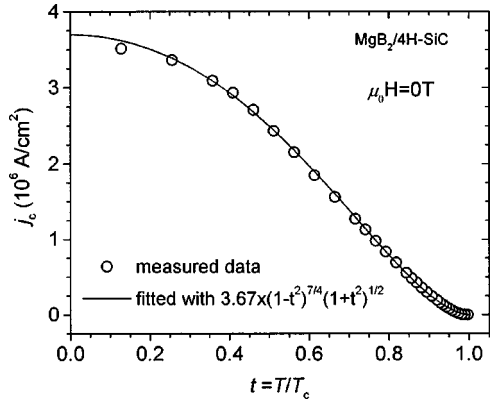

FIG. 3. Plots of the j_c-T data measured with fine temperature steps at zero external field with 4-probe method for a sample on 4H-SiC. It shows the common features with a positive curvature at $T \rightarrow T_c$, a nearly linear part in the central range of temperature and a negative curvature when $T \rightarrow 0$ K. The solid line is a fit with $3.67 \times 10^6 \times (1-t^2)^{7/4}(1+t^2)^{1/2}$, where $t = T/T_c$.

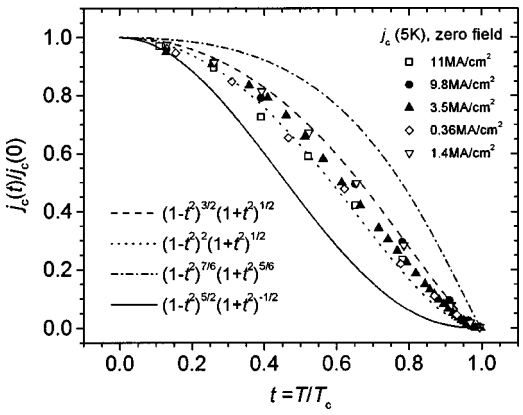

FIG. 4. Different MgB_2 films show similar normalized *j-t* scaling where $j(t) = j_c(t)/j_c(0)$, although their corresponding $j_c(0)$ varies from 10^7 A/cm^2 to 10^5 A/cm^2. The data locate in a narrow band defined by $j(t) = (1-t^2)^{3/2}(1+t^2)^{1/2}$ and $(1-t^2)^2(1+t^2)^{1/2}$.

B. Scaling of normalized *j-t*

The data plotted in Fig. 3 can be well fitted with $j_c(t) = j_c(0)(1-t^2)^{\alpha}(1+t^2)^{1/2}$, where $t = T/T_c$ is the reduced temperature, $\alpha = 7/4$, $T_c = 39.1$ K and $j_c(0) = 3.7 \times 10^6$ A/cm^2 for this sample. This scaling behavior of j_c in temperature is similar to that observed in conventional low-T_c superconductors such as Sn microbridges, where for a spatially uniform current flow, $j_c(t) \approx j_c(0)(1-t^2)^{3/2}(1+t^2)^{1/2}$.[22] Indeed we note that $j_c(t) = j_c(0)(1-t^2)^{\alpha}(1+t^2)^{1/2}$ works well for the $j_c(T)$ data of all the samples, where individually $\alpha = 1.7 \pm 0.1$ for the data measured with the 4-probe method and $\alpha \approx 2$ for the data derived from the *M-H* loops. In Fig. 4 we plotted the data measured with the 4-probe method of five different samples with their fitted $j_c(0)$ values varying in three orders of magnitude from 10^7 A/cm^2 to 10^5 A/cm^2. Most of their normalized $j(t) \equiv j_c(t)/j_c(0)$ fall to a narrow band confined by two $j(t) = (1-t^2)^{\alpha}(1+t^2)^{1/2}$ curves with $\alpha = 3/2$ and 2, respectively.

For type-II superconductors one may find clues of the general pinning mechanism from their $j_c(T)$ behavior in temperature. It has been demonstrated that by using generalized inversion scheme (GIS)[24,25] one can distinguish δl-pinning or δT_c-pinning in high-T_c superconducting thin films with a scaling law of $j(t) = (1-t^2)^{5/2}(1+t^2)^{-1/2}$, or $j(t) = (1-t^2)^{7/6}(1+t^2)^{5/6}$, respectively.[25] Here δl-pinning and δT_c-pinning refer to the pinning results from disorders in the mean free path l, and in the transition temperature T_c, respectively.[26] Griessen *et al.* concluded from the fitting results that δl-pinning mechanism is dominant in $YBa_2Cu_3O_7$ and $YBa_2Cu_4O_8$ thin films.[25] By using similar analyses on the magnetization data of MgB_2, it was argued that δT_c-pinning mechanism is dominant in sintered bulk[27] and thin films.[10] For the current films, as shown in Fig. 4, the experimental data points are between the two fitting curves corresponding to δl- and δT_c-pinning, respectively. This scaling behavior suggests that both δl-pinning and δT_c-pinning play roles in the epitaxial MgB_2 thin films made by HPCVD. Clearly the δT_c-pinning is not dominant in the present films, consistent with the fact that the present films

have a very pure superconducting phase by showing a higher T_c and a narrower ΔT_c in comparison with that previously reported.

For a superconductors, the depairing current density and the thermodynamic critical field can be estimated by $j_0 = 4B_c/[3\sqrt{6}\mu_0\lambda]$ and $B_c = \Phi_0/[2\sqrt{2}\pi\lambda\xi]$, respectively,[26] where λ is the penetration depth, and $\Phi_0 = h/2e$ is the flux quantum, and ξ is the coherence length. For MgB_2, by taking $\lambda_{ab}(0) \sim 100-110$ nm[28,29] and $\xi_{ab}(0) \sim 5-7$ nm,[7] j_0 and B_c are estimated to be $\sim 2\times 10^8$ A/cm^2 and ~ 0.35 T, respectively. The best j_c values of the present films at low temperature is in the order of 10^7-10^8 A/cm^2, fulfill well the criterion for the strong vortex pinning regime, $j_c/j_0 \sim 0.1-1$.[26] Thus the scaling behavior on temperature observed in the present films may indicate the existence of strong pinning forces in the films caused by extended defects. As discussed in the following section, such extended defects are most likely formed in the columnar boundaries along the *c* axis during the growth of the present films.[4,17]

C. Field dependence of j_c

For MgB_2 superconductors, it has been demonstrated that grain boundaries do not cause remarkable decrease of j_c,[30,31] therefore the $j_c(H)$ behavior is mainly determined by the nature of vortex state and vortex pinning of the materials. In low perpendicular magnetic fields and low temperatures, $j_c(H)$ exhibits a plateau in field less than H^*, which is nearly temperature independent, as typically shown in the inset of Fig. 5(a). The $\mu_0 H^*$ values are found to be $\sim 10^{-2}$ T. By performing initial *M-H* measurements of the films, we have found that in perpendicular fields, magnetic flux starts to penetrate into the films at $\mu_0 H_a \sim 2.5 \pm 0.3$ mT, corresponding to a lower critical field $\mu_0 H_{c1}$ of 20–25 mT when the demagnetization of the films is considered. In the external fields $H_a < H < H^*$, the vortex pinning in the films is described under the ideal single vortex regime.[26] In MgB_2 powders, similar behavior was observed,[30] while the $\mu_0 H^*$ values are $\sim 10^{-1}$ T at low temperatures.

With further increase of *H*, a nearly linear region appears in the double logarithmic plot of the j_c-*H* data, as shown in Fig. 5(b) and Fig. 5(c), indicating a power dependence of j_c on *H*. The $j_c(H)$ curves show a transition at a crossover field, here referred to as H_m. When the external field is less than $\mu_0 H_m \sim 1$ T [in Figs. 5(b) and 5(c)], $j_c(H) \propto H^{-\beta}$ where $\beta \sim 0.7-1.0$. When $H > H_m$, $j_c(H)$ decreases nearly exponentially with the field.

The power dependence of $j_c(H)$ observed here is very similar to that observed in high-T_c cuprate thin films consisting of linear defects as strong pinning sites.[32,33] In epitaxial YBCO thin films, strong pinning sites in the grain boundaries lead to a power dependence $j_c(H) \propto H^{-\beta}$ with $\beta \sim 0.5$,[32] and linear dislocations in the films lead to a $\beta \sim 0.5-1.1$[33] in moderate perpendicular fields. For the latter, clear correlations among β, H^*, and the dislocation density n_{disl}, revealed by continuous wet etching and atomic force microscopy mapping, have been observed.[33]

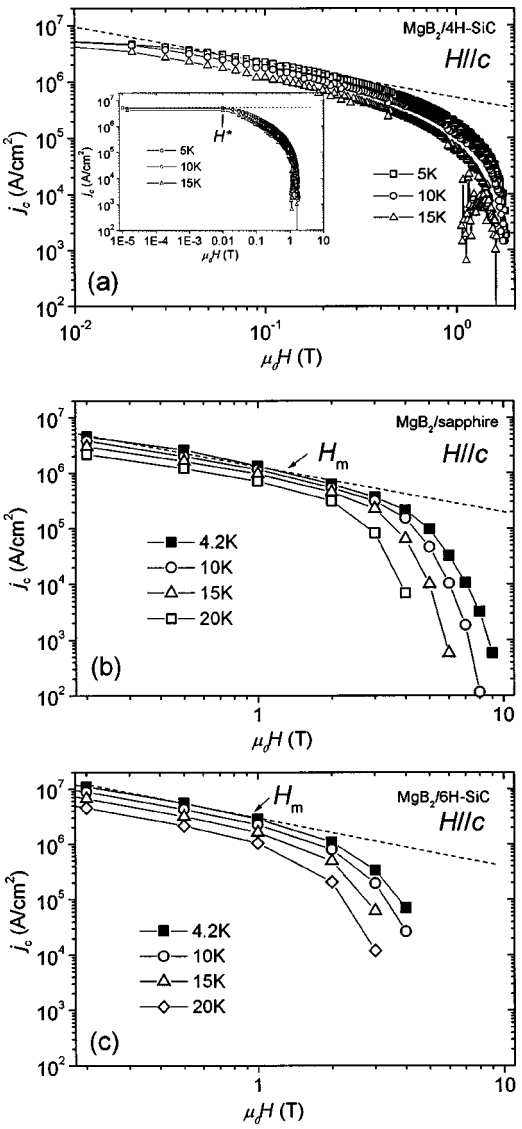

FIG. 5. Critical current density $j_c(H)$ data in perpendicular external field ($H \| c$) of three MgB_2 epitaxial films: (a) a 180 nm thick sample on 4H-SiC, derived from *M-H* loops with the Bean model, (b) a 290 nm thick sample on sapphire, measured with 4-probe method, and (c) a 92 nm thick sample on 6H-SiC, measured with 4-probe method. The inset of (a) shows a plateau at low fields. (b) and (e) show the $j_c(H)$ behavior in high fields, where j_c turns from power dependence to exponential dependence in increasing fields. The dashed lines are guides to the eye.

Considering both the fact of $j_c/j_0 \sim 0.1-1$ and the power dependence of $j_c(H)$ in fields, vortex pinning revealed in the present films could be explained under the framework for strong vortex pinning.[26] The turning fields from the plateau to a power slope at low temperature might correspond to the bundle field B_{rb} for strong pinning, above which, the vortices are in the plastic pinning or collective pinning regime.[26] Schönenberger *et al.*[34] have shown that $\beta = 0.7 \pm 0.1$ for $j_c(H) \propto H^{-\beta}$ can be derived from simulations using the model of plastic deformation due to strong pinning. In the region $H_m < H < H_{\mathrm{irr}}$, the $j_c(H)$ curve deviates from the power dependence and decreases steeply, where the small or

large bundle pinning are possibly dominant in the vortex pinning.[26]

From transmission electron microscopy (TEM) and atomic force microscopy analyses,[4,17] we have revealed that the present films consist of columnar grains with flat top surfaces. It leads to a natural speculation that most of the strong pinning centers in these films are located at the column boundaries. With columnar growth mode, planes of the column boundaries are parallel to the *c*-axis of the film. In perpendicular field where $H \| c$, once a vortex is pinned it is expected that the vortex line be pinned along its whole length within the column boundary, thus presenting a strong pinning force. Looking back to the field H_m, we find it in the same order as the in-plane matching fields for the geometry lattices formed by the uniform hexagonal columns of the films. For example, the films for Figs. 5(b) and 5(c) have an average in-plane column dimension ~100 nm.[17] Considering identical in-plane hexagonal shape of these columns, the length of each edge of the hexagons is thus $100/\sqrt{3} \sim 60$ nm, and we obtain a matching flux density $B_\phi \sim 0.7$ T for a triangular vortex lattice as that observed in MgB_2 single crystals.[35] In the films on sapphire, the H_m value is usually larger than that of the films on SiC. This is probably due to more defects induced by the large lattice mismatch between sapphire and MgB_2, causing the existence of twin boundaries.[4] The perfect lattice matching between MgB_2 and SiC in the *ab* plane (-0.5%)[5] naturally makes the entire film on SiC more single-crystal-like with better intercolumn connection and few defects, as compared to those on sapphire, resulting in a higher zero-field j_c but a poorer sustainability of j_c in fields. The weaker sustainability of $j_c(H)$ in high fields suggests a lack of a high density of pinning centers for vortex pinning,[26] consistent with the single-crystal-like crystalline quality of the films.[4]

The above discussions generally classify the vortices pinned in the films into two sorts: those strongly pinned at the column boundaries (and twin boundaries as well in films on sapphire), and those weakly pinned in the single-crystal-like bodies of the columns. The latter have a much higher chance to creep locally, or jump over to neighboring strong pinning sites and form small bundles. The weak sustainability of j_c of the films in high fields is attributed to the lack of a high density of point defects in the present films.

The irreversibility field $H_{\rm irr}$ are roughly estimated from $j_c(T,H)$ and $\rho(T,H)$ data obtained with 4-probe measurements, where the criteria of $j_c(T,H)=10^3$ A/cm^2 and $\rho(T,H)/\rho_n=10^{-3}$ are applied for the estimation, respectively, similar to those used for MgB_2 bulk,[30] thin film[15] and single crystal[19] for a reasonable comparison. The current density 10^3 A/cm^2 is considered as the same level of thermal noises.[30] At the vicinity where resistivity of the films appears, the resistivity values increase steeply in temperature in $\log \rho$-T plots, as shown in Fig. 1. At $\rho(T,H)/\rho_n=10^{-4}$ the data are already in the noise background (this part is not shown in Fig. 1), and the temperature differences between that corresponding to $\rho(T,H)/\rho_n=10^{-3}$ and $\rho(T,H)/\rho_n=10^{-2}$ are mostly in the order of 0.1 K under various field. Therefore the criterion $\rho(T,H)/\rho_n=10^{-3}$ gives reasonable estimation of $H_{\rm irr}$ data. For the same film, both methods give similar results. Figure 6 presents two sets of typical $H_{\rm irr}$ data measured from two microbridge samples of films on SiC and sapphire. The films on SiC tend to show lower $H_{\rm irr}$ values than those on sapphire due to a better crystallinity. The H_{c2} values in $H \| c$ estimated at 90% of ρ_n from $\rho(T,H)$ curves of the same samples are also plotted in Fig. 6 for a comparison. One sees here a small gap between $H_{\rm irr}$ and H_{c2} for the present films, which is in sharp contrast to the large gap observed[15] in the *c*-axis MgB_2 thin films made by the two-step approach.[2]

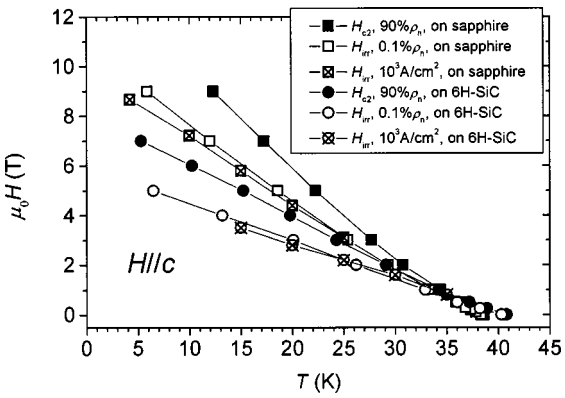

FIG. 6. The irreversibility field $H_{\rm irr}$ in perpendicular fields $(H \| c)$, derived from $\rho(T,H)$ and $j_c(T,H)$ data measured with 4-probe method from two films on sapphire and 6H-SiC, respectively. The fields at $j_c(T,H)=10^3$ A/cm^2 and $\rho(T,H)/\rho_n=10^{-3}$ are defined here as the $H_{\rm irr}$ values, respectively. The H_{c2} values of these samples, estimated at 90%ρ_n from the $\rho(T,H)$ data, are also plotted for reference. All lines are guides to the eye.

D. Magnetic flux jump induced effects

As just discussed, it is expected that vortices in the films are weakly pinned in the single-crystal-like bodies of the columns and easy to creep locally or jump over to neighboring strong pinning sites. When a number of such jumps occur at the same time, it would result in an observable macroscale change in the transport properties of the films. In magnetization measurements, as shown in Fig. 7, flux-jump induced peaks in *M*-*H* loops repeatedly appear at the same fields, regardless of the change of temperature from 5 K to 15 K. This implies that the flux jump is mainly determined structurally, not thermally, and the thermal activation energy for vortex depinning is very high in the films.

Much higher flux jump induced magnetization peaks in *M*-*H* loops at low field have been reported in Mg-diffused thin films,[14] MgB_2 sintered bulks[36] and wires.[37] Severe suppression of the nominal j_c at temperature lower than 10–15 K was reported in these samples.[12,14] It has been argued and demonstrated that in polycrystalline MgB_2 materials the samples were not uniform and dentritic penetration of vortices occurred.[12,38]

By contrast, under low fields the present *in situ* epitaxial MgB_2 thin films have not shown a suppression of the nominal j_c in the *M*-*H* loops with a temperature down to 4.2 K. We attribute it to the uniform and excellent crystalline microstructures of the films. However, we repeatedly observe

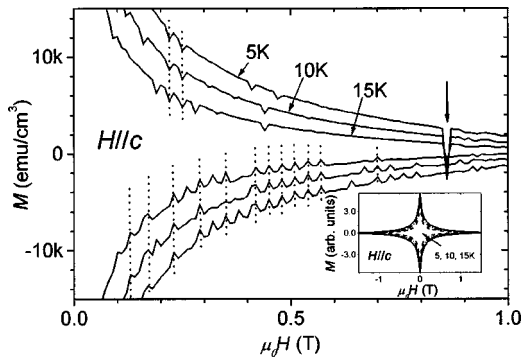

FIG. 7. Magnetization hysteresis curves measured from a 110 nm thick film grown on 4H-SiC, with a field step of 10 mT and a sweeping rate $d(\mu_0 H)/dt = 2$ mT/s. Many small peaks, probably flux jump induced, are observed. These peaks occur at the same fields (marked with dotted lines and an arrow as guides to the eye) when temperature varies. The inset shows the full loops.

flip-over jumps in the *M-H* loops when the maximum field is high (e.g., 3–5 T) and the field-sweeping rate is high (e.g., 10 mT/s), as shown in Fig. 8. For both films on sapphire and SiC the flip-over field was around 0.85 T, and does not shift in varied temperature from 5 K to 15 K. It once again implies strong structurally but not thermally pinning characteristics of the present films. The loss of hysteresis in the *M-H* loops when the field is larger than the flip-over field indicates the collapse of the normal pinning mechanism; probably dentritic penetration of vortices has occurred in this regime.[38] When the external field is less than the flip-over field, an

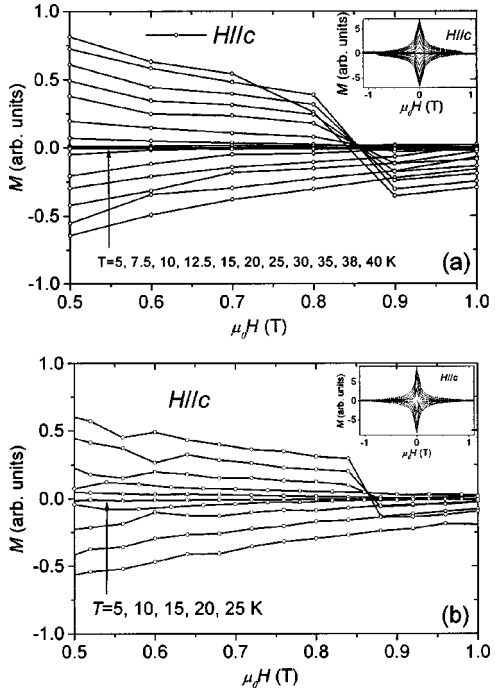

FIG. 8. Magnetization hysteresis curves from (a), a 110 nm thick MgB_2 epitaxial film on 4H-SiC with a field sweeping rate $d(\mu_0 H)/dt = 10$ mT/s and a field step of 100 mT, and (b) a 220 nm thick MgB_2 film on sapphire with a field sweeping rate of 5 mT/s and a field step of 40 mT. The insets show the full loops.

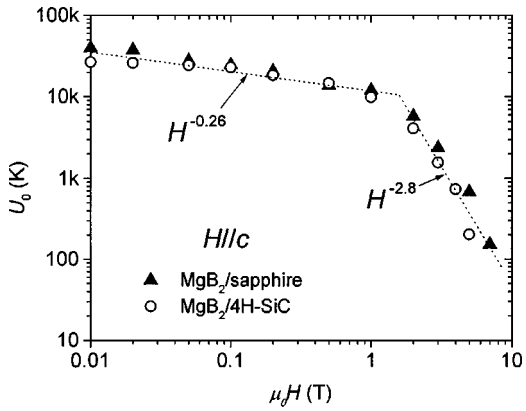

FIG. 9. Thermal activation energy derived from $\rho(H,T)$ data of two MgB_2 thin films on sapphire and 4H-SiC, respectively, in perpendicular fields. The data follow some power dependences to the field, i.e., $U \propto H^{\nu}$, with turning fields around 1.5 T where U decreases much faster with H. The dotted lines are guides to the eye.

overall supercurrent is recovered in the film and vortices are pinned again sufficiently, and the magnetization moment flips over to follow the ''normal'' *M-H* loops. Such phenomenon has also been observed in the measurements of our *in situ* MgB_2 films made by pulsed laser deposition.[39] The role of the sweeping rate of field in the flux jumping mechanism is to be further studied, e.g., by relaxation measurement.

The temperature independent flux jumps observed in the *M-H* loops are consistent with the large values of the thermal activation energy $U_0(H,T)$ derived from Arrhenius plots of the sample resistivity, $\rho(H,T) = \rho_0 \exp[-U_0(H,T)/k_B T]$, where ρ_0 is a fitting parameter and k_B the Boltzman constant. We find that U_0 is three orders of magnitude higher than $k_B T_c$, as shown in Fig. 9. Similar to those observed in high-T_c single crystals,[40] in both perpendicular and parallel fields, a power dependence $U \propto H^{-\nu}$ and a turning field where ν steeply increases are observed. For example, in $H \| c$, ν increases from ~ 0.26 to ~ 2.8 when the fields cross the turning point ~ 1.5 T for two films on sapphire and SiC, respectively (Fig. 9). The origin of this phenomenon is not yet clear.

IV. CONCLUSION

In summary, the *in situ* epitaxial MgB_2 thin films grown on (0001) sapphire and SiC by HPCVD technique show single-crystal-like epitaxial textures and excellent transport properties in terms of high T_c, narrow ΔT_c and high zero-field j_c. The best zero-field j_c is comparable to the depairing current density of MgB_2. The zero-field $j_c(T)$ values of different films show a common trend and can be scaled to $j(t) = (1-t^2)^{\alpha}(1+t^2)^{1/2}$, where $\alpha = 1.7 \pm 0.1$ for the data measured with the 4-probe method and $\alpha \approx 2$ for the data derived from the *M-H* loops. Films on both sapphire and SiC show weak sustainability in moderate perpendicular fields. At low temperature the j_c of the films show a common feature, i.e., $j_c(H)$ first appears as a plateau when the external field is lower than H^*, where $\mu_0 H^* \sim 10^{-2}$ T, and then $j_c(H) \propto H^{-\beta}$ when the field is lower than a crossover value H_m, where $\beta \sim 0.7$–1.0 and $\mu_0 H_m \sim 1$ T. Above H_m, $j_c(H)$

decreases steeply. The power dependence of $j_c(H) \propto H^{-\beta}$ is similar to that observed in epitaxial high-T_c cuprate films with a density of linear defects as strong pinning sites. These results indicate the existence of extended defects in the present MgB_2 thin films. Considering the microstructure of the films, we suggest that the strong pinning centers are mainly located in the column boundaries, which are formed during the columnar growth of the films. We also observed nearly temperature independent small peaks and flip-over in *M-H* hysteresis loops of the films, which might be related to the creeping behavior of the weakly pinned vortices that penetrate in the single-crystal-like columns. This implies a high thermal activation energy $U_0(H,T)$ of the films, consistent with the derived $U_0(H,T)$ values from Arrhenius plots of the resistivity measurements.

The weak sustainability of j_c in high magnetic fields might be improved by introducing a high density of impurity or defects into the films;[9,41,42] such approaches are under investigation.

ACKNOWLEDGMENTS

The work is partially supported by NSF under Grant No. DMR-9876266 & Petroleum Research Fund (Q.L.), and by ONR under Grant No. N00014-00-1-0294 (X.X.X.). J.M.R. thanks the financial support by ONR Grant No. N0014-01-1-0006.

*Email: benxusy@psu.edu

[1] J. Nagamatsu, N. Nakagawa, T. Muranaka, Y. Zenitani, and J. Akimitsu, Nature (London) **410**, 63 (2001).
[2] W. N. Wang, H. J. Kim, E. M. Choi, C. U. Jung, and S. I. Lee, Science **292**, 1521 (2001).
[3] S. H. Moon, J. H. Yun, H. N. Lee, J. I. Kye, H. G. Kim, W. Chung, and B. Oh, Appl. Phys. Lett. **79**, 2429 (2001).
[4] X. H. Zeng, A. V. Pogrebnyakov, A. Kotcharov, J. E. Jones, X. X. Xi, E. M. Lysczek, J. M. Redwing, S. Y. Xu, Q. Li, J. Lettieri, D. G. Schlom, W. Tian, X. Q. Pan, and Z. K. Liu, Nature Mater. **1**, 35 (2002).
[5] X. H. Zeng, A. V. Pogrebnyakov, M. H. Zhu, J. E. Jones, X. X. Xi, S. Y. Xu, E. Wertz, Qi Li, J. M. Redwing, L. Lettieri, V. Vaithyanathan, D. G. Schlom, Z. K. Liu, O. Trithaveesak, and Schubert, Appl. Phys. Lett. **82**, 2097 (2003).
[6] X. X. Xi, X. H. Zeng, A. V. Pogrebnyakov, S. Y. Xu, Q. Li, Yu Zhong, C. O. Brubaker, Zi-Kui Liu, E. M. Lysczek, J. M. Redwing, J. Lettieri, D. G. Schlom, W. Tian, and X. Q. Pan, IEEE Trans. Appl. Supercond. **13**, 3233 (2003).
[7] C. Buzea and T. Yamashita, Supercond. Sci. Technol. **14**, R115 (2001).
[8] J. Rowell, Nature Mater. **1**, 5 (2002).
[9] C. B. Eom, M. K. Lee, J. H. Choi, L. J. Belenky, X. Song, L. D. Cooley, M. T. Naus, S. Patnaik, J. Jiang, M. Rikel, A. Polyanskii, A. Gurevich, X. Y. Cai, S. D. Bu, S. E. Babcock, E. E. Hellstrom, D. C. Larbalestier, N. Rogado, K. A. Regan, M. A. Hayward, T. He, J. S. Slusky, K. Inumaru, M. K. Haas, and R. J. Cava, Nature (London) **411**, 558 (2001).
[10] S. L. Prischepa, M. L. Della Rocca, L. Maritato, M. Salvato, R. Di Capua, M. G. Maglione, and R. Vaglio, Phys. Rev. B **67**, 024512 (2003).
[11] S. K. Gupta, S. Sen, N. Joshi, D. K. Aswal, I. K. Gopalakrishnan, J. V. Yakhmi, V. C. Sahni, E. M. Choi, K. H. P. Kim, H. S. Lee, H. J. Kim, W. N. Kang, and S. I. Lee, Physica C **385**, 313 (2003).
[12] H. J. Kim, W. N. Wang, E. M. Choi, M. S. Kim, K. H. P. Kim, and S. I. Lee, Phys. Rev. Lett. **87**, 087002 (2001).
[13] S. K. Gupta, S. Sen, A. Singh, D. K. Aswal, J. V. Yakhmi, E. M. Choi, H. J. Kim, K. H. P. Kim, S. Choi, H. S. Lee, W. N. Kang, and S. I. Lee, Phys. Rev. B **66**, 104525 (2002).
[14] Z. W. Zhao, S. L. Li, Y. M. Ni, H. P. Yang, Z. Y. Liu, H. H. Wen, W. N. Kang, H. J. Kim, E. M. Choi, and S. I. Lee, Phys. Rev. B **65**, 064512 (2001).
[15] H. H. Wen, S. L. Li, Z. W. Zhao, H. Jin, Y. M. Ni, W. N. Kang, H. J. Kim, E. M. Choi, and S. I. Lee, Phys. Rev. B **64**, 134505 (2001).
[16] S. D. Bu, D. M. Kim, J. H. Choi, J. Giencke, E. E. Hellstom, D. C. Larbalestier, S. Patnaik, L. Cooley, C. B. Eom, J. Lettieri, D. G. Schlom, W. Tian, and X. Q. Pan, Appl. Phys. Lett. **81**, 1851 (2002).
[17] S. Y. Xu, A. V. Pogrebnyakov, X. H. Zeng, J. E. Jones, Qi Li, J. M. Redwing, and X. X. Xi (unpublished).
[18] A. V. Pogrebnyakov, J. M. Redwing, J. E. Jones, X. X. Xi, S. Y. Xu, Qi Li, V. Vaithyanathan, and D. J. Schlom, Appl. Phys. Lett. **82**, 4319 (2003).
[19] Yu. Eltsev, S. Lee, K. Nakao, N. Chikumoto, S. Tajima, N. Koshizuka, and M. Murakami, Physica C **378–381**, 61 (2002).
[20] U. Welp, A. Rydh, G. Karapetrov, W. K. Kwok, G. W. Crabtree, Ch. Marcenat, L. Paulius, T. Klein, J. Marcus, K. H. P. Kim, C. U. Jung, H. S. Lee, B. Kang, and S. I. Lee, Phys. Rev. B **67**, 012505 (2003).
[21] C. Ferdeghini, V. Ferrando, V. Braccini, M. R. Cimberle, D. Marré, P. Manfrinetti, A. Palenzona, and M. Putti, Eur. Phys. J. B **30**, 147 (2003).
[22] W. J. Skocpol, Phys. Rev. B **14**, 1045 (1976).
[23] G. Stejic, A. Gurevich, E. Kadyrov, D. Christen, R. Joynt, and D. C. Larbalestier, Phys. Rev. B **49**, 1274 (1994).
[24] H. G. Schnack, R. Griessen, J. G. Lensink, and Wen Hai-hu, Phys. Rev. B **48**, 13 178 (1993).
[25] R. Griessen, Wen Hai-hu, A. J. J. van Dalen, J. Rector, H. G. Schnack, S. Libbrecht, E. Osquiguil, and Y. Bruynseraede, Phys. Rev. Lett. **72**, 1910 (1994).
[26] G. Blatter, M. V. Feigel'man, V. B. Geshkenbein, A. I. Larkin, V. M. Vinokur, Rev. Mod. Phys. **66**, 1125 (1994).
[27] M. J. Qin, X. L. Wang, H. K. Liu, and S. X. Dou, Phys. Rev. B **65**, 132508 (2001).
[28] Ch. Niedermayer, C. Bernhard, T. Holden, P. K. Kremer, and K. Ahn, Phys. Rev. B **65**, 094512 (2002).
[29] F. Manzano, A. Carrington, N. E. Hussey, S. Lee, A. Yamamoto, and S. Tajima, Phys. Rev. Lett. **88**, 047002 (2002).
[30] Y. Bugoslavsky, G. K. Perkins, X. Qi, L. F. Cohen, and A. D. Caplin, Nature (London) **410**, 563 (2001).
[31] D. C. Larbalestier, L. D. Cooley, M. O. Rikel, A. A. Polyanskii, J. Jiang, S. Patnaik, X. Y. Cai, D. M. Feldmann, A. Gurevich, A. A. Squitieri, M. T. Naus, C. B. Eom, E. E. Hellstrom, R. J. Cava, K. A. Regan, N. Rogado, M. A. Hayward, T. He, J. S. Slusky, P. Khalifah, K. Inumaru, and M. Haas, Nature (London) **410**, 186 (2001).

[32] A. Dfiaz, L. Mechin, P. Berghuis, and J. E. Evetts, Phys. Rev. Lett. **80**, 3855 (1998).
[33] B. Dam, J. M. Huijbregtse, F. C. Klaassen, R. C. F. van der Geest, G. Doornbos, J. H. Rector, A. M. Testa, S. Freisem, J. C. Martinez, B. Stauble-Pumpin, and R. Griessen, Nature (London) **399**, 439 (1999); F. C. Klaassen, G. Doornbos, J. M. Huijbregtse, R. C. F. van der Geest, B. Dam, and R. Griessen, Phys. Rev. B **64**, 184523 (2001).
[34] A. Schönenberger, A. Larkin, E. Heeb, V. Geshkenbein, and G. Blatter, Phys. Rev. Lett. **77**, 4636 (1996).
[35] L. Ya. Vinnikov, J. Karpinski, S. M. Kazakov, J. Jun, J. Anderegg, S. L. Bud'ko, and P. C. Canfield, Phys. Rev. B **67**, 092512 (2003).
[36] S. X. Dou, X. L. Wang, J. Horvat, D. Milliken, A. H. Li, K. Konstantinov, E. W. Collings, M. D. Sumption, and H. K. Liu, Physica C **361**, 79 (2001).
[37] S. Jin, H. Mavoori, C. Bower, and R. B. van Dover, Nature (London) **411**, 563 (2001).
[38] T. H. Johansen, M. Baziljevich, D. V. Shantsev, P. E. Goa, Y. M. Galperin, W. N. Kang, H. J. Kim, E. M. Choi, M. S. Kim, and S. I. Lee, Europhys. Lett. **59**, 599 (2002); M. Baziljevich, A. V. Bobyl, D. V. Shantsev, E. Altshuler, T. H. Johansen, and S. I. Lee, Physica C **369**, 93 (2002); F. L. Barkov, D. V. Shantsev, T. H. Johansen, P. E. Goa, W. N. Kang, H. J. Kim, E. M. Choi, M. S. Kim, and S. I. Lee, Phys. Rev. B **67**, 064513 (2003).
[39] X. H. Zeng, A. Sukiasyan, X. X. Xi, Y. F. Hu, E. Wertz, Qi Li, W. Tian, H. P. Sun, X. Q. Pan, J. Lettieri, D. G. Schlom, C. O. Brubaker, Z. K. Liu, and Qiang Li, Appl. Phys. Lett. **79**, 1840 (2001).
[40] T. T. M. Palstra, B. Batlogg, L. F. Schneemeyer, and J. V. Waszczak, Phys. Rev. Lett. **61**, 1662 (1988); T. T. M. Palstra, B. Batlogg, R. B. van Dover, L. F. Schneemeyer, and J. V. Waszczak, Phys. Rev. B **41**, 6621 (1990).
[41] J. Wang, Y. Bugoslavsky, A. Berenov, L. Cowey, A. D. Caplin, L. F. Cohen, J. L. M. Driscoll, L. D. Cooley, X. Song, and D. C. Larbalestier, Appl. Phys. Lett. **81**, 2026 (2002).
[42] Y. Bugoslavsky, L. F. Cohen, G. K. Perkins, M. Polichetti, T. J. Tate, R. Gwilliam, and A. D. Caplin, Nature (London) **411**, 561 (2001).